HHS Public Access

Author manuscript

Mucosal Immunol. Author manuscript; available in PMC 2016 March 01.

Published in final edited form as:

Mucosal Immunol. 2015 September ; 8(5): 1118–1130. doi:10.1038/mi.2015.3.

Deficiency of autophagy protein Map1-LC3b mediates IL-17-dependent lung pathology during respiratory viral infection via ER stress associated IL-1

Michelle Reed[1], **Susan H. Morris**[1], **Anna B. Owczarczyk**[1], and **Nicholas W. Lukacs**[1,2]

[1]Department of Pathology, University of Michigan Medical School, Ann Arbor, MI 48109

Abstract

While recent studies suggest that IL-1β production is modulated by macroautophagy or sensors of ER stress upon pro-inflammatory insult, autophagy and IL-1β production during viral infection has not been fully investigated. This was addressed using respiratory syncytial virus (RSV), which is associated with lung immunopathology, IL-1, and IL-17a secretion in severely infected patients. Mice deficient in the autophagy-associated protein Map1-LC3b (LC3b$^{-/-}$) developed increased IL-17a-dependent lung pathology upon infection. RSV-infected LC3b$^{-/-}$ DCs fail to upregulate autophagosome formation, secrete IL-1β and IL-6, and elicit IL-17a production from CD4+ T cells. Bone marrow chimeras revealed both structural and hematopoietic LC3b deficiency contribute to the development of IL-17a-dependent lung pathology *in vivo*. Further investigation revealed airway epithelium as the primary source of IL-1β during infection, while inhibition of the ER-stress sensor IRE-1 in primary airway epithelial cells reduced IL-1β production identifying a primary ER stress pathway. Finally, blockade of IL-1 receptor signaling in RSV-infected LC3b$^{-/-}$ mice abolished IL-17a-dependent lung pathology. These findings provide novel mechanistic insight into the contribution of autophagy- and ER stress-dependent cytokine production that initiate and maintain aberrant Th17 responses, while identifying IL-1 as a potential therapeutic target in the treatment of severe respiratory viral infections.

Introduction

Human respiratory syncytial virus (RSV) remains the leading cause of infant hospitalization in the United States [1,2], and is responsible for considerable morbidity among infants, the elderly, and individuals with chronic respiratory illnesses worldwide [3–5]. Hospitalization with RSV as an infant is also highly correlated with the development of recurrent wheezing in childhood, suggesting lasting immune environment alteration in the lung post-infection [6]. The severity of lower-respiratory tract RSV infection in otherwise healthy individuals is largely driven by an over-exuberant immune response to the virus, and is characterized by bronchiolitis, epithelial cell sloughing, mucus hyper-secretion, and infiltration of neutrophils

[2]Corresponding author: Nicholas W Lukacs, 109 Zina Pitcher Place, 4059 BSRB, Department of Pathology, University of Michigan, Ann Arbor, MI 48109-2200. nlukacs@umich.edu, tel (734)764-5135.

The authors declare no conflict of interest at this time.

into the airways [7,8]. Elevated levels of the pro-inflammatory cytokines IL-1, IL-6 and IL-17a have recently been noted in respiratory aspirate samples from patients hospitalized with severe RSV infections [9–11], while experimental evidence suggests that IL-17a production drives mucus hypersecretion, neutrophil infiltration, and the suppression of CD8+ T cell responses in the context of RSV infection [10,12,13]. The mechanisms by which Th17 immune responses to RSV are initiated and maintained remains poorly understood.

Within the lung environment, resident dendritic cells (DCs) detect invading pathogens and mediate both innate and adaptive immune responses through cytokine secretion and antigen presentation to T cells. Classical induction of IL-17a production by murine CD4+ T cells requires expression of the innate cytokines IL-6 and TGFβ by antigen-presenting cells (APCs), while IL-23 is required for the expansion and survival of Th17 cells [14,15]. In contrast, the induction of IL-17a secretion by human CD4+ T cells requires IL-1 and IL-6 but not TGFβ [16], while IL-1 receptor signaling is required for the production of IL-17a by both human and mouse CD4+ T cells [17]. The production of IL-23 by DCs in response to TLR ligands is further driven by IL-1β [18], suggesting a critical role for IL-1 in the maintenance of Th17 responses.

The IL-1 family proteins IL-1β and IL-18 are synthesized upon TLR activation in an inactive precursor state, and regulated via post-translational cleavage by assembled inflammasome complexes such as AIM2 and NLRP3 [19]. The secretion of IL-1β and IL-18 by DCs and macrophages upon TLR activation is also negatively regulated by macroautophagy (autophagy), a homeostatic mechanism by which cytosolic constituents are enveloped in a double-walled membrane and delivered to lysosomes for degradation. Pro-IL-1β and pro-IL-18 are rapidly sequestered within autophagosomes upon the induction of autophagy [20], while ubiquitinated inflammasomes are bound by sequestosome-1/p62 and selectively targeted to nascent autophagosomes through p62 binding to membrane-bound Map-1LC3b (LC3b)[21]. It was recently reported that RSV infection activates the NLRP3 inflammasome and induces IL-1β secretion from human bronchial epithelial cells [22], as well as murine macrophages and epithelial cells [23]. Our laboratory has found evidence supporting a critical role for autophagy in DCs by promoting activation, cytokine secretion, and antigen presentation upon RSV infection in vitro [24], while autophagy deficiency in DCs enhances RSV-induced pathology in vivo [25]. However, the potential modulatory role of autophagy in controlling excessive inflammasome activation and IL-1β secretion during RSV infection has yet to be examined.

Since RSV infects via a membrane fusion event that allows direct entry of its genetic material into the cytoplasm, activation of critical innate TLR responses rely on autophagy to transport viral PAMPs and promote appropriate anti-viral responses [24]. To investigate the potential role of autophagy in mitigating RSV-induced lung pathology *in vivo*, mice deficient in the critical autophagy protein LC3b (LC3b$^{-/-}$) were used. These mice have been previously reported to express greater NLRP3 inflammasome activation, IL-1β secretion, and increased susceptibility to experimental sepsis [26]. Our results demonstrate that LC3b is critical to the regulation of Th17-induced lung pathology during RSV infection, as LC3b$^{-/-}$ mice show greater mucus hypersecretion, lung neutrophil infiltration, and IL-17a production, which was ameliorated by IL-17a neutralization. These disease-associated

pathologies were associated with increased IL-1β and IL-6 production in the LC3b deficient mice during RSV infection that were related to ER stress responses based upon specific pathway blockade. Importantly, blockade of IL-1 receptor signaling *in vivo* substantially reduced IL-17a secretion and immunopathology in the lungs of LC3b$^{-/-}$ mice, suggesting a potential therapeutic approach to alleviating severe RSV-induced responses.

Results

I. LC3b$^{-/-}$ mice develop increased IL-17a-dependent lung pathology upon RSV infection

As development of severe RSV infection in humans is characterized by bronchiolitis, mucus hypersecretion, and neutrophil accumulation in the lungs [], these parameters were assessed in RSV-infected LC3b$^{-/-}$ mice at 8 days post infection. Lung histological sections stained with haematoxylin and eosin (H & E) revealed greater peribronchial edema and granulocyte infiltration into lungs of RSV-infected LC3b$^{-/-}$ mice, in comparison to WT littermate controls (Figure 1A). Additionally, greater periodic acid-schiff (PAS)-positive mucus staining was visible along the apical epithelial surface of the major airways of RSV-infected LC3b$^{-/-}$ mice (Figure 1A), while mRNA transcripts for the mucus-associated genes *muc5ac* and *gob5* were elevated in the lungs of RSV-infected LC3b$^{-/-}$ mice (Figure 1B). In order to assess lung viral replication, qPCR for mRNA transcripts encoding the RSV-G and –F proteins was performed on whole lung homogenates. This revealed increased viral transcripts in the lungs of infected LC3b$^{-/-}$ mice, which suggests decreased viral clearance relative to WT littermates (Figure 1C). Finally, in agreement with our histological findings, significantly higher numbers of neutrophils were detected in the lungs of RSV-infected LC3b$^{-/-}$ mice by flow cytometry (Figure 1D).

Experimental evidence has shown a causative role for T cell-associated cytokines, most recently IL-17a, in the development of severe lung pathology during RSV infection [10]. Whole-lung lysates from RSV-infected LC3b$^{-/-}$ mice revealed greater IL-17a protein production in comparison to littermate controls (Figure 1E). Conversely, lung mRNA expression of IFNγ was significantly lower in comparison to littermate controls (Figure 1F). The presence of IL-1, IL-6, and TGFβ are required for the induction of mucosal Th17 responses in mice [15,17], and indeed, lung protein levels of IL-1α, IL-1β, and IL-6 were elevated in whole lung lysates from RSV-infected LC3b$^{-/-}$ mice (Figure 1G). In contrast, no differences were detected in lung mRNA expression of TGFβ, while lung protein levels of the inflammasome-dependent cytokine IL-18 did not differ between LC3b$^{-/-}$ mice and WT littermates (data not shown). Finally, mediastinal lymph node (MedLN) cell cultures were restimulated *ex vivo* with RSV and demonstrated that LC3b$^{-/-}$ cultures secreted significantly greater amounts of IL-17a in comparison to WT cultures (Figure 1H).

Previous studies found that CD4+ T cells are the predominant source of IL-17a in the lungs of WT mice at 8 days post-RSV infection []. However, recent advances in other IL-17-dependent disease models indicate that γδ-T cell receptor-positive T cells and innate lymphoid cells (ILCs) produce large quantities of IL-17a in response to IL-1 receptor signaling. In order to determine which cell types were responsible for elevated IL-17a production in LC3b$^{-/-}$ mice, intracellular staining and flow cytometry were performed on lung digests and MedLN cells from RSV-infected LC3b$^{-/-}$ mice. While the numbers of γδ-

receptor-positive T cells and ILC3 cells positive for IL-17a were increased in the lungs of LC3b$^{-/-}$ mice in comparison to WT littermates, the majority of IL-17a-positive cells were CD4+ T cells (Figure 1I). Significantly greater numbers of IL-17a-positive CD4+ T cells were also detected in MedLNs of LC3b$^{-/-}$ mice (Figure 1J), suggesting that increased production of IL-17a by CD4+ T cells are primarily responsible for elevated IL-17a levels in both the lungs and MedLNs of RSV-infected LC3b$^{-/-}$ mice.

Previous studies conducted by our laboratory found that IL-17a production contributes to lung inflammation, excessive mucus production, and the suppression of IFNγ production by CD8+ T cells during RSV infection [10,27]. To assess whether the increased lung pathology in RSV-infected LC3b$^{-/-}$ mice was IL-17a-dependent, LC3b$^{-/-}$ mice were treated with neutralizing antibodies to IL-17a. In comparison to control antibody treatment, administration of anti-IL-17a antibodies to RSV-infected LC3b$^{-/-}$ mice substantially decreased visible lung inflammation and leukocyte infiltration at 8 days post-infection (Figure 2A). Neutralization of IL-17a significantly decreased PAS-positive mucin staining along the bronchial epithelium, which was verified by decreased *muc5ac* expression in lungs of anti-IL-17a-treated LC3b$^{-/-}$ mice at 8 days post-infection (Figure 2A, 2B). Neutralization of IL-17a also reduced the neutrophil accumulation in the LC3−/− mice (Figure 2C). Remarkably, neutralization of IL-17a rescued viral clearance in LC3b−/− mice, as anti-IL-17a-treated LC3b−/− mice showed lung viral mRNA levels equivalent to WT controls (Figure 2D). Lung IFNγ expression was also significantly higher in comparison to control-antibody treated LC3b−/− mice corresponding to a more effective cellular immune response (Figure 2E). These results collectively suggest that the development of increased lung pathology in LC3b$^{-/-}$ mice is IL-17a-dependent.

II. Altered autophagy, innate cytokine production, and CD4+ T cell cytokine elicitation by LC3b$^{-/-}$ CD11b+ DCs in response to RSV infection

Recent work identified a requirement for CD11c^{high} CD11b+ tissue-resident DCs in the induction of mucosal Th17 immune responses [28,29]. As pharmacological blockade of autophagy increases IL-23 secretion by DCs and macrophages in response to TLR agonists [18], the ability of LC3b$^{-/-}$ DCs to upregulate autophagosome formation and secrete innate cytokines in response to RSV was investigated. Confocal microscopy revealed robust formation of ATG5+ autophagosomes by WT bone marrow-derived DCs (BMDCs) in response to RSV infection (Figure 3A). In contrast, LC3b$^{-/-}$ BMDCs failed to increase formation of ATG5+ puncta in response to RSV (Figure 3A). In agreement with these observations, levels of the sequesteosome protein p62 decreased in whole-cell lysates of WT BMDCs by 8 hours post-infection, while LC3b$^{-/-}$ BMDCs continued to accumulate p62 over a 24 hr period (Figure 3B). Analysis of cytokine secretion by RSV-infected BMDCs revealed significantly higher production of IL-1β and IL-6 by LC3b$^{-/-}$ BMDCs (Figure 3C). LC3b$^{-/-}$ BMDCs expressed less of the IL-12-specific subunit IL-12p35 and the IL-12/IL-23 common subunit IL-12p40 by qPCR, in comparison to WT BMDCs (Figure 3D). Conversely, RSV-infected LC3b$^{-/-}$ BMDC significantly upregulated IL-23p19 expression in comparison to WT BMDCs (Figure 3D). These findings were confirmed using CD11c^{high} CD11b^{+} lamina propria DCs (CD11b^{+} LP DCs), flow-sorted from lungs of naïve WT and LC3b$^{-/-}$ mice that were infected *ex vivo* with RSV. LC3b$^{-/-}$ CD11b^{+} LP DCs secreted

greater amounts of IL-1β and IL-6 upon RSV infection, while IL-12p35 and IL-12p40 mRNA expression were significantly reduced in comparison to WT controls (Figure 3E, 3F). In order to assess whether LC3b$^{-/-}$ DCs preferentially elicit increased IL-17a secretion from CD4+ T cells in response to RSV infection, BMDCs were co-cultured with purified CD4+ T cells derived from MedLNs of RSV-infected WT mice. CD4+ MedLN T cells secreted significantly greater quantities of IL-17a in co-culture with RSV-infected LC3b$^{-/-}$ BMDCs, in comparison to T cells co-cultured with infected WT BMDCs (Figure 3G). To further investigate DC elicitation of CD4+ T cell IL-17a secretion as a consequence of autophagy deficiency, purified CD4+ splenic OT-II T cells were co-cultured with BMDCs pulsed with ovalbumin protein. These latter studies were conducted in the presence or absence of RSV in order to provide an autophagic stimulus, as ovalbumin treatment alone does not induce autophagy. While co-cultures in which WT and LC3b$^{-/-}$ DCs were treated with ovalbumin alone produced similar quantities of IL-17a, cultures in which LC3b$^{-/-}$ DCs were concurrently infected with RSV elicited significantly greater IL-17a production from the CD4+ OT-II T cells (Figure 3H). These findings were confirmed using CD11b^{+} LP DCs isolated from lungs of naïve WT and LC3b$^{-/-}$ mice, with RSV-infected and ovalbumin-pulsed LC3b$^{-/-}$ CD11b^{+} LP DCs eliciting significantly higher quantities of IL-17a from co-cultured OT-II T cells (Figure 3I). These results support impaired autophagy and altered innate cytokine production by LC3b$^{-/-}$ DCs as primary mechanisms in the initiation of Th17-skewed CD4+ T cell responses to RSV infection.

III. Non-Immune cell deficiency in LC3b augments Th17-associated RSV pathology through increased IL-1 secretion by airway epithelial cells

Results thus far indicated that LC3b$^{-/-}$ CD11b+ DCs elicit increased IL-17a production from CD4+ T cells in response to RSV. As LC3b expression in epithelial cells is an important modulator of lung pathology upon exposure to cigarette smoke [30] or hyperoxia [31], bone marrow chimeric mice were created to assess relative contributions of structural and hematopoietic cells to observed RSV-induced lung pathology. Histologic examination of lung tissue 8 days post-infection revealed that WT mice reconstituted with LC3b$^{-/-}$ bone marrow experienced significant increases in lung inflammation, infiltration of neutrophils, and IL-17a production in comparison to fully WT chimeric animals (Figure 4A–C), suggesting that hematopoietic LC3b deficiency is sufficient to induce increased IL-17 production and neutrophil infiltration in response to RSV *in vivo*. Interestingly, reconstitution of LC3b$^{-/-}$ mice with WT bone marrow produced an augmented inflammatory response, as significantly higher numbers of neutrophils were found in the lungs in comparison to all other treatment groups (Figure 4B). These PMN accumulation data correlated well with analysis that revealed augmented production of IL-17a in lung tissues and restimulated MedLN cultures (Figure 4C, 4D), with the WT to LC3b$^{-/-}$ chimera having the most significant effect. Lung expression of IFNγ was inversely correlated with IL-17a production (Figure 4E), while IL-6 expression was associated with structural LC3b deficiency (Figure 4F). Finally, investigation of innate cytokine concentrations in the lungs of chimeric mice revealed increased IL-1α and IL-1β in lung lysates of RSV-infected LC3b$^{-/-}$ chimeric mice, independent of WT or LC3b$^{-/-}$ bone marrow reconstitution (Figure 4D), implicating structural cells as the primary source of these cytokines in the lungs. These findings suggest that while LC3b$^{-/-}$ bone marrow is sufficient for the development of

increased Th17-dependent lung pathology in response to RSV, LC3b$^{-/-}$ lung structural cells contribute to the development of pathology through increased secretion of innate cytokines.

IV. Airway Epithelial cells deficient in LC3b have enhanced inflammasome activation and increased cytokine production due to ER Stress

To further examine innate cytokine production in response to RSV, fluorescent immunohistochemistry was used to examine IL-1β protein expression in lung sections of infected mice. This revealed greater staining intensity in lungs of RSV-infected LC3b$^{-/-}$ mice, with the vast majority of IL-1β-positive cells co-staining for the epithelial marker E-Cadherin (Figure 5A). To verify these findings, primary airway epithelial cell (AEC) cultures were derived from lungs of naïve mice and infected with RSV *in vitro*. In agreement, LC3b$^{-/-}$ AEC cultures upregulated IL-1β and IL-6 mRNA and secreted greater quantities of protein upon RSV infection, in comparison to WT cultures (Figure 5B, 5C). While IL-1α mRNA was upregulated in RSV-infected LC3b$^{-/-}$ AECs (Figure 5B), IL-1α was not detected in culture supernatants, possibly due to a lack of cell lysis in culture (data not shown). As LC3b$^{-/-}$ macrophages were also reported to secrete greater quantities of IL-1β in response to inflammasome-activating stimuli [26], the expression of IL-1β by lung-infiltrating immune cells was examined by flow cytometry. This revealed greater intensity of IL-1β staining in LC3b$^{-/-}$ lung macrophages in response to RSV infection (Figure 5D), suggesting that these cells may also contribute to elevated IL-1β levels in lungs of LC3b$^{-/-}$ mice.

RSV infection is a known inducer of ER stress and NLRP3 inflammasome activation in bronchial epithelial cells [22,32]. As prolonged ER stress reportedly triggers NLRP3 inflammasome activation [33], the expression levels of several genes activated during ER stress were examined in RSV-infected AEC cultures. In agreement with the previous report of signaling through the ER stress-sensing receptor IRE-1α upon RSV infection [32], mRNA expression of Edem-1 and cleaved XBP-1 (XBP-1s) were significantly elevated in RSV-infected LC3b$^{-/-}$ AEC cultures at 12 hours post-infection (Figure 5E). Furthermore, pre-treatment of LC3b$^{-/-}$ AECs with the IRE-1α inhibitor 3,5-dibromosalicylaldehyde (DBSA) reduced the secretion of IL-1β and IL-6 to levels comparable to WT AECs (Figure 5F). Finally, in order to assess the contribution of ER stress to inflammasome activation during RSV infection, expression of the active p10 subunit of caspase-1 was measured in primary AEC cultures infected with RSV. Confocal imaging and fluorescence quantification of caspase-1 p10 antibody staining revealed increased signal in LC3b$^{-/-}$ AECs 12 hours post-treatment with RSV, in comparison to WT control cultures (Figure 5G). Pre-treatment of LC3b$^{-/-}$ AECs with DBSA abolished this difference (Figure 5G). Collectively, these results suggest that elevated RSV-induced production of IL-1β and IL-6 by the LC3b$^{-/-}$ airway epithelium is due to increased inflammasome activation and ER stress, and may have a critical role in shaping the ongoing immune response during RSV infection.

V. Blockade of IL-1 receptor signaling ameliorates IL-17a-associated pathology in LC3b$^{-/-}$ mice *in vivo*

In order to assess whether excessive IL-1 production was driving the development of the elevated Th17 response in LC3b$^{-/-}$ mice, murine IL-1 receptor antagonist (IL-1Ra) was

administered immediately prior to and during the course of RSV infection. Strikingly, LC3b$^{-/-}$ mice treated with IL-1Ra during RSV infection showed substantially reduced peribronchial inflammation in comparison to LC3b$^{-/-}$ saline treatment controls (Figure 6A). Treatment with IL-1Ra decreased PAS-positive mucus in the airways of RSV-infected LC3b$^{-/-}$ mice (Figure 6A, lower panels), which was verified through significantly reduced mRNA expression of muc5ac in lung homogenates (figure 6B). Quantification of lung neutrophils by flow cytometry revealed decreased neutrophil infiltration in IL-1Ra-treated LC3b$^{-/-}$ mice, in comparison to saline-treated controls (Figure 6C). Examination of cytokine production in lungs by qPCR revealed significantly reduced IL-17a expression in IL-1Ra-treated LC3b$^{-/-}$ mice, with a concomitant increase in IFNγ production in response to RSV infection (Figure 6D). Finally, IL-17a secretion by MedLN cells restimulated *ex vivo* was significantly reduced in cultures from LC3b$^{-/-}$ mice who received IL-1Ra treatment (Figure 6E). These results ultimately suggest that elevated IL-17a production and associated lung pathology in RSV-infected LC3b$^{-/-}$ mice are driven by IL-1 receptor signaling.

Discussion

In this manuscript, we provide evidence for the importance of the autophagy protein LC3b in both innate cytokine production and the induction of adaptive immune responses to RSV. Mice deficient in LC3b developed greater IL-17a-dependent lung pathology upon RSV infection, characterized by neutrophil infiltration, mucus hypersecretion, and decreased viral clearance in comparison to WT littermates. The identification of CD4+ T cells as the predominant IL-17a-positive cell type in LC3b$^{-/-}$ lungs at 8 days post-RSV infection concurs with previous studies in wild-type mice[10], and implicates enhanced DC-mediated induction of Th17 responses in the subsequent development of lung pathology. In agreement with previous work showing a requirement for autophagy in innate cytokine production and antigen presentation by DCs [18,24], RSV-infected LC3b$^{-/-}$ DCs produced IL-1β, IL-6, and IL-23 at the expense of IL-12 and preferentially elicited IL-17a production from CD4+ T cells (Figure 7A). This preferential induction of Th17 responses to RSV was further evidenced by the development of elevated lung pathology in WT chimeric mice reconstituted with LC3b$^{-/-}$ bone marrow. However, LC3b$^{-/-}$ chimeras reconstituted with WT bone marrow developed an augmented Th17 response to RSV, possibly due to both a robust induction of CD4+ T cell responses by WT DCs, with elevated IL-17a production occurring in response to the high-IL-1 environment of LC3b$^{-/-}$ lungs (Figure 7B). Indeed, infected LC3b$^{-/-}$ airway epithelial cells secreted greater amounts of IL-1β in a manner dependent on elevated IRE-1α signaling. Finally, treatment of LC3b$^{-/-}$ mice with IL-1Ra attenuated IL-17a production and associated lung pathology in response to RSV, implicating enhanced IL-1 receptor signaling in the development of IL-17-driven lung pathology. The identification of these innate pathways may lead to new strategies to alleviate pathophysiologic changes during RSV infection that lessen severity and subsequent long term sequelae of pulmonary damage associated with RSV.

Since the discovery of Th17 cell lineage, aberrant or excessive Th17 immune responses have been found to enhance pathology in the context of immune-mediated disorders such as rheumatoid arthritis [34] and allergic asthma [35], as well as during viral infection [36]. Studies of severe RSV infection suggest that a Th17-skewed response contributes to lung pathology in

at least a subset of patients, as elevated IL-17a expression has been reported in tracheal aspirates of infants hospitalized with RSV [10,37]. In addition, lung expression of IL-6 and IL-1 are correlated with severity of disease in both infants and adults infected with RSV [9,38]. In the present studies treatment of LC3b$^{-/-}$ mice with anti-IL-17a antibodies during RSV infection significantly decreased lung neutrophil infiltration and mucus hypersecretion, while also elevating lung IFNγ expression and restoring viral clearance. IL-17a may drive lung pathology by inducing mucus gene expression [39], potentiating IL-8 production in RSV-infected bronchial epithelial cells, thereby augmenting lung neutrophil recruitment [37], or by suppressing cytotoxic CD8+ T cell activity [10] and prolonging infection. This is supported by previous findings in our laboratory, as administration of neutralizing antibodies to IL-17a attenuated lung mucus production and neutrophil infiltration [10,28]. The recovery of IFNγ production in LC3b$^{-/-}$ mice treated with anti-IL-17a antibodies is also likely due to a reduction in IL-17a, as IL-17a also suppresses the production of IFNγ and cytotoxic molecules by CD8+ T cells *in vivo*[10]. Moreover, *in vivo* blockade of IL-1 receptor signaling through IL-1Ra treatment mitigated lung production of IL-6 and IL-17a in RSV-infected LC3b$^{-/-}$ mice, resulting in reduced lung pathology. While our data cannot rule out a lack of viral clearance as an explanation for increased pathology, the findings do provide further evidence in support of the critical role of LC3-dependent autophagy secretion during infectious insult [26], as well as novel evidence supporting the role of autophagy in counteracting deleterious Th17 responses to RSV through blocking inflammasome-mediated production of IL-1β.

The production of IL-23 by DCs and macrophages is also indirectly regulated by autophagy, through autophagy-mediated inhibition of IL-1 secretion [18]. The alteration of autophagy reduces the ability to shuttle RSV RNA to endosomic TLR pathways, which have been shown to be associated with regulation of IL-23 and IL-17a [28]. Accordingly, we found that RSV-infected LC3b$^{-/-}$ DCs that failed to upregulate autophagosome formation secreted more IL-1β, IL-6, and IL-23, and preferentially induced IL-17a expression from co-cultured CD4+ T cells in comparison to WT controls. Experiments with chimeric mice further support a causative role for autophagy deficiency in DC-mediated induction of Th17 responses to RSV, as WT mice reconstituted with LC3b$^{-/-}$ bone marrow developed similar lung pathology as mice fully deficient in LC3b. Conversely, the development of T cell-dependent lung pathology in fully LC3b$^{-/-}$ mice may be dampened not only by inefficient antigen presentation by autophagy-deficient DCs [40,41], but may also be due to a requirement for autophagy proteins in the survival and proliferation of effector T cells [42,43]. In support of this, the reconstitution of LC3b$^{-/-}$ mice with WT bone marrow augmented Th17-dependent lung pathology above levels observed in fully LC3b$^{-/-}$ mice. Ultimately, these results suggest critical roles for LC3b-dependent autophagy in both structural and hematopoietic cells in mitigating inflammasome activation and the development of Th17-associated lung pathology during RSV infection.

Several non-exclusive mechanisms may contribute to increased IL-1β secretion by LC3b$^{-/-}$ DCs, macrophages, and airway epithelial cells in response to RSV infection. Our findings of increased IL-1β secretion and active caspase-1 by LC3b$^{-/-}$ AECs concurs with two recent reports of RSV infection inducing IL-1β secretion in macrophages [23] and primary human

airway epithelial cells [22] through an NLRP3- and caspase-1-dependent mechanism. While LC3b-dependent autophagy directly regulates inflammasome activity in macrophages through selective degradation of ubiquitinated NLRP3 inflammasome platforms [21] and pro-IL-1β [20], further work will be required to establish this mechanism in epithelial cells during RSV infection. The inability of LC3b$^{-/-}$ cells to regulate inflammasome activation through autophagy may be further exacerbated by an inability to remove damaged mitochondria through mitophagy [26]. Reactive oxygen species released by damaged mitochondria are required for NLRP3 inflammasome activation and caspase-1-mediated IL-1β production [44,45], and this was recently verified in RSV-infected macrophages [23]. Autophagy-deficient LC3b$^{-/-}$ macrophages accumulated damaged mitochondria and mitochondrial ROS in response to LPS and ATP treatment, resulting in greater NLRP3 inflammasome activation and IL-1β secretion [26]. As RSV infection was previously reported to increase numbers of morphologically altered mitochondria in human airway epithelial cells [46], an inability to sequester damaged mitochondria via LC3b-associated mechanisms may contribute to increased inflammasome activation upon infection.

Importantly, these data uncovered evidence of increased ER stress in LC3b$^{-/-}$ AECs upon RSV infection. Recent data indicated that RSV infection of A549 cells activates ER stress response signaling through IRE-1 and ATF6 [32]. ER stress is known to upregulate pro-survival autophagy [47,48], while numerous studies have shown a requirement for IRE-1 pathway signaling in the regulation of autophagy during the ER stress response [47,49]. It was also recently reported that the induction of ER stress activates the NLRP3 inflammasome and increases IL-1β secretion in a manner dependent on mitochondrial integrity [33]. It is therefore plausible that ER stress in RSV-infected cells may serve the dual purpose of promoting cell survival through autophagy-mediated removal of viral nucleic acids and proteins, while simultaneously controlling NLRP3 inflammasome activation through degradation of damaged mitochondria and assembled inflammasome platforms. Further studies will be required to elucidate the exact mechanisms underlying increased RSV-induced inflammasome activation and IL-1β secretion by LC3b$^{-/-}$ cells.

These findings provide additional evidence for the role of autophagy during RSV infection in promoting the induction of antiviral Th1 responses to RSV *in vivo*. Furthermore, these results suggest that LC3b associated responses and autophagy serves as a critical negative regulator of inflammation during RSV infection, through limitation of IL-1β production by lung epithelial cells. The present studies highlight the unique, cell-specific contribution of autophagy proteins to inflammatory processes, and provide valuable insight into the induction and development of Th17-skewed responses during RSV infection. Ultimately, this information may inform novel treatments for severe RSV infection, and ultimately aid in vaccine design strategies.

Materials and Methods

Mice

Female C57Bl/6J and B6.Cg-Tg(TcraTcrb)425Cbn/J (OT-II) mice were purchased from The Jackson Laboratory (Bar Harbor, ME). B6;129P2-*Map1lc3b*^{tm1Mrab}/J were obtained from The Jackson Laboratory and repeatedly backcrossed to C57Bl/6J mice to produce WT or

LC3b-deficient ($LC3b^{-/-}$) mice of ≥98% C57Bl/6 background. All *in vivo* experiments utilized age- and sex-matched WT or $LC3b^{-/-}$ littermates. Bone marrow chimeras were created by irradiating WT or $LC3b^{-/-}$ littermates at 900rad, followed by tail-vein injection of 2×10^6 whole bone marrow cells of the genotype indicated. Chimeras were allowed to reconstitute for 8 weeks prior to RSV infection. All work involving animals was conducted in accordance with University of Michigan Committee on Use and Care of Animals policy.

Respiratory Syncytial Virus

All experiments utilized antigenic subgroup A, Line 19 strain RSV, originally isolated from a sick infant in the University of Michigan Health System. Viral stocks were maintained in Hep-2 cell cultures.

Dendritic Cell Isolation and Culture

Bone marrow-derived dendritic cells (BMDCs) were cultured in complete media as previously described [25], from whole bone marrow in the presence of 20ng/ml GM-CSF (R&D Systems, Minneapolis, MN). Lung-resident CD11b+ and CD103+ DCs were isolated by enzymatic digestion of lungs of naïve WT or $LC3b^{-/-}$ mice as previously described [25]. Briefly, minced lung tissue was incubated with 200μg/ml Liberase TM (Roche Applied Science, Indianapolis, IN) and 200U/ml DNase I (Sigma-Aldrich), drawn through an 18-gauge needle, and filtered through 40μm mesh. Cells were positively selected for CD11c expression using anti-mouse CD11c microbeads and magnetic column separation (Miltenyi Biotec, Auburn CA), followed by staining with PE-labeled anti-CD11b and allophycocyanin-labeled anti-CD103 Abs (eBioscience, San Diego, CA). Cells were sorted on an iCyt Synergy 3200 fluorescence-activated cell sorter (Champaign, IL), followed by overnight culture in complete media.

For DC-T cell co-culture experiments, RSV-responsive CD4+ T cells were obtained from mediastinal lymph nodes of RSV-infected C57Bl/6J mice, 8 days post-infection. CD4+ OT-II T cells were isolated from minced spleens of OT-II transgenic mice. Cells were purified using a magnetic column negative-selection protocol, yielding untouched CD4+ T cells (Miltenyi Biotec). CD4+ T cells were added to culture at a 10:1 ratio to DCs. For RSV-reactive T cell co-cultures, DCs were infected with 1:1 MOI RSV 2 hours prior to the addition of T cells. For OT-II T cell co-cultures, DCs were treated with 200μg/ml whole ovalbumin protein, or concurrently treated with ovalbumin and 1:1 MOI of RSV, for 2 hours prior to the addition of T cells. Culture supernatants were harvested at 48 hours and analyzed using a custom BioRad Bioplex PRO kit on a BioRad Bioplex 200 system, according to manufacturer instructions (BioRad).

Airway Epithelial Cell culture

Airway epithelial cell cultures were prepared from lungs of naïve mice by digestion in Dispase (BD Biosciences), followed by filtration through 25μm nylon mesh. Immune cells were depleted using biotinylated anti-CD45 antibodies and streptavidin-conjugated Dynabeads (Thermo Fisher Scientific). Cells were plated on 10cm tissue culture dishes and adherence-purified in DMEM-based complete media, followed by 4 day culture in fibronectin-coated wells.

Reagents

Recombinant mouse IL-1Ra was obtained from R&D systems. Neutralizing antibodies to mouse IL-17a were generated and purified in-house, as described previously [10]. The ER stress inhibitors 3,5-dibromosalicylaldehyde and 4-phenylbutyrate were purchased from Santa Cruz Biotechnology.

Quantitative PCR

Total RNA was isolated from cell cultures and lung tissue using TRIzol reagent, according to manufacturer's instructions (Invitrogen). RNA was reverse-transcribed, and cytokine gene expression was assessed using TaqMan Gene Expression Assay primer/probe sets on an ABI Prism 7500 Sequence Detection System (Applied Biosystems, Foster City, CA). Custom primers were used to assess transcription levels of *muc5ac*, *gob5*, *RSV-G* and *RSV-F*, as previously described [50]. Fold change expression was calculated from gene expression values normalized to GAPDH, relative to the indicated control group.

Flow Cytometry

Cells were isolated from the right lungs and mediastinal LNs by digestion in 200μg/ml Liberase TM (Roche Applied Science, Indianapolis, IN) and 200U/ml DNase I (Sigma-Aldrich). Cells were stained with Live/Dead Fixable Yellow (Invitrogen), followed by fluorescent antibodies as indicated. Analysis was performed using FlowJo software (TreeStar, Ashland OR).

Immunofluorescence and Confocal Microscopy

BMDCs and AECs were cultured as described above, and plated in Labtek chamber slides (Thermo Fisher Scientific). After indicated treatment, cells were fixed in 4% paraformaldehyde, followed by blocking in DPBS containing 5% normal goat serum and 0.1% Tween-20. Cells were stained with DyLight 550-conjugated anti-ATG5 antibodies (Novus Biologicals, Littleton, CO), or rabbit anti-Caspase-1 p10 (Santa Cruz Biotechnologies) followed by AlexaFluor 488-conjugated goat anti-rabbit antibodies (Jackson ImunoResearch, West Grove, PA). Slides were mounted in ProLong Gold antifade reagent plus DAPI, and imaged using 40× oil immersion objective on a Nikon A1 Confocal Microscope System using NIS Elements software (Nikon Instruments). Maximum intensity projection images were generated using ImageJ software (National Institutes of Health).

For fluorescent immunohistochemistry. formalin-fixed paraffin-embedded lung sections were de-parrafinized, rehydrated, and incubated overnight in antigen retrieval buffer (0.01M Citric acid, pH 6.0). Slices were blocked in DPBS + 2% normal goat serum, followed by incubation with rabbit anti-mouse IL-1β (Novus Biologicals, Littleton, CO) and biotinylated anti-E-cadherin (BD Biosciences). After washing in blocking buffer, slices were incubated with anti-rabbit Alexa Fluor 568 and streptavidin-conjugated Alexa Fluor 488 (BD Biosciences). Images were taken using a 40× objective on an Olympus BX43 fluorescent microscope.

Statistics

Data were analyzed and graphed using GraphPad Prism software. Statistical significance was determined by one-way ANOVA and Bonferroni post-test to obtain p values.

Acknowledgements

We would like to acknowledge the editing assistance of Dr. Judith Connett, technical assistance provided by Dr. Matthew Schaller, and histological slide preparation by Lisa Riggs Johnson. We also thank the Flow Cytometry and Microscopy Imaging and Analysis Core Facilities at the University of Michigan. This work was supported by NIH-HL-114858.

References

1. Leader S, Kohlhase K. Recent trends in severe respiratory syncytial virus (RSV) among US infants, 1997 to 2000. J. Pediatr. 2003; 143:S127–S132. [PubMed: 14615711]
2. Stockman LJ, Curns AT, Anderson LJ, Fischer-Langley G. Respiratory syncytial virus-associated hospitalizations among infants and young children in the United States, 1997–2006. Pediatr. Infect. Dis. J. 2012; 31:5–9. [PubMed: 21817948]
3. Falsey AR, Hennessey PA, Formica MA, Cox C, Walsh EE. Respiratory syncytial virus infection in elderly and high-risk adults. N. Engl. J. Med. 2005; 352:1749–1759. [PubMed: 15858184]
4. Tan WC. Viruses in asthma exacerbations. Curr. Opin. Pulm. Med. 2005; 11:21–26. [PubMed: 15591884]
5. Wedzicha JA. Role of viruses in exacerbations of chronic obstructive pulmonary disease. Proc. Am. Thorac. Soc. 2004; 1:115–120. [PubMed: 16113423]
6. Sigurs N, et al. Severe respiratory syncytial virus bronchiolitis in infancy and asthma and allergy at age 13. Am. J. Respir. Crit. Care Med. 2005; 171:137–141. [PubMed: 15516534]
7. Drunen Littel-van den Hurk S, van & Watkiss ER. Pathogenesis of respiratory syncytial virus. Curr. Opin. Virol. 2012; 2:300–305. [PubMed: 22709517]
8. Johnson JE, Gonzales RA, Olson SJ, Wright PF, Graham BS. The histopathology of fatal untreated human respiratory syncytial virus infection. Mod. Pathol. 2006; 20:108–119. [PubMed: 17143259]
9. Duncan CB, Walsh EE, Peterson DR, Lee FE-H, Falsey AR. Risk factors for respiratory failure associated with respiratory syncytial virus infection in adults. J. Infect. Dis. 2009; 200:1242–1246. [PubMed: 19758094]
10. Mukherjee S, et al. IL-17-induced pulmonary pathogenesis during respiratory viral infection and exacerbation of allergic disease. Am. J. Pathol. 2011; 179:248–258. [PubMed: 21703407]
11. Tabarani CM, et al. Novel inflammatory markers, clinical risk factors and virus type associated with severe respiratory syncytial virus infection. Pediatr. Infect. Dis. J. 2013; 32:e437–e442. [PubMed: 23804121]
12. Bera MM, et al. Th17 Cytokines Are Critical for Respiratory Syncytial Virus-Associated Airway Hyperreponsiveness through Regulation by Complement C3a and Tachykinins. J. Immunol. 2011; 187:4245–4255. [PubMed: 21918196]
13. Ryzhakov G, et al. IL-17 Boosts Proinflammatory Outcome of Antiviral Response in Human Cells. J. Immunol. 2011; 187:5357–5362. [PubMed: 21964025]
14. Bettelli E, et al. Reciprocal developmental pathways for the generation of pathogenic effector TH17 and regulatory T cells. Nature. 2006; 441:235–238. [PubMed: 16648838]
15. Mangan PR, et al. Transforming growth factor-beta induces development of the T(H)17 lineage. Nature. 2006; 441:231–234. [PubMed: 16648837]
16. Acosta-Rodriguez EV, Napolitani G, Lanzavecchia A, Sallusto F. Interleukins 1beta and 6 but not transforming growth factor-beta are essential for the differentiation of interleukin 17-producing human T helper cells. Nat. Immunol. 2007; 8:942–949. [PubMed: 17676045]
17. Hu W, Troutman TD, Edukulla R, Pasare C. Priming microenvironments dictate cytokine requirements for T helper 17 cell lineage commitment. Immunity. 2011; 35:1010–1022. [PubMed: 22137454]

18. Castro, CPde, et al. Autophagy regulates IL-23 secretion and innate T cell responses through effects on IL-1 secretion. J. Immunol. 2012; 189:4144–4153. [PubMed: 22972933]
19. Latz E, Xiao TS, Stutz A. Activation and regulation of the inflammasomes. Nat. Rev. Immunol. 2013; 13:397–411. [PubMed: 23702978]
20. Harris J, et al. Autophagy controls IL-1β secretion by targeting pro-IL-1β for degradation. J. Biol. Chem. 2011; 286:9587–9597. [PubMed: 21228274]
21. Shi C-S, et al. Activation of autophagy by inflammatory signals limits IL-1β production by targeting ubiquitinated inflammasomes for destruction. Nat. Immunol. 2012; 13:255–263. [PubMed: 22286270]
22. Triantafilou K, Kar S, Vakakis E, Kotecha S, Triantafilou M. Human respiratory syncytial virus viroporin SH: a viral recognition pathway used by the host to signal inflammasome activation. Thorax. 2013; 68:66–75. [PubMed: 23229815]
23. Segovia J, et al. TLR2/MyD88/NF-κB Pathway, Reactive Oxygen Species, Potassium Efflux Activates NLRP3/ASC Inflammasome during Respiratory Syncytial Virus Infection. PLoS ONE. 2012; 7:e29695. [PubMed: 22295065]
24. Morris S, et al. Autophagy-mediated dendritic cell activation is essential for innate cytokine production and APC function with respiratory syncytial virus responses. J. Immunol. Baltim. Md 1950. 2011; 187:3953–3961.
25. Reed M, et al. Autophagy-Inducing Protein Beclin-1 in Dendritic Cells Regulates CD4 T Cell Responses and Disease Severity during Respiratory Syncytial Virus Infection. J. Immunol. 2013; 191:2526–2537. [PubMed: 23894198]
26. Nakahira K, et al. Autophagy proteins regulate innate immune responses by inhibiting the release of mitochondrial DNA mediated by the NALP3 inflammasome. Nat. Immunol. 2011; 12:222–230. [PubMed: 21151103]
27. Lukacs NW, et al. Respiratory virus-induced TLR7 activation controls IL-17-associated increased mucus via IL-23 regulation. J. Immunol. Baltim. Md 1950. 2010; 185:2231–2239.
28. Schlitzer A, et al. IRF4 Transcription Factor-Dependent CD11b+ Dendritic Cells in Human and Mouse Control Mucosal IL-17 Cytokine Responses. Immunity. 2013; 38:970–983. [PubMed: 23706669]
29. Persson EK, et al. IRF4 transcription-factor-dependent CD103(+)CD11b(+) dendritic cells drive mucosal T helper 17 cell differentiation. Immunity. 2013; 38:958–969. [PubMed: 23664832]
30. Chen Z-H, et al. Autophagy protein microtubule-associated protein 1 light chain-3B (LC3B) activates extrinsic apoptosis during cigarette smoke-induced emphysema. Proc. Natl. Acad. Sci. 2010; 107:18880–18885. [PubMed: 20956295]
31. Tanaka A, et al. Hyperoxia-induced LC3B interacts with the Fas apoptotic pathway in epithelial cell death. Am. J. Respir. Cell Mol. Biol. 2012; 46:507–514. [PubMed: 22095627]
32. Hassan I, et al. The Inositol Requiring Enzyme 1 Inhibits Respiratory Syncytial Virus Replication. J. Biol. Chem. 2014
33. Menu P, et al. ER stress activates the NLRP3 inflammasome via an UPR-independent pathway. Cell Death Dis. 2012; 3:e261. [PubMed: 22278288]
34. Bedoya SK, Lam B, Lau K, Larkin J 3rd. Th17 cells in immunity and autoimmunity. Clin. Dev. Immunol. 2013; 2013:986789. [PubMed: 24454481]
35. Wang Y-H, Wills-Karp M. The potential role of interleukin-7 in severe asthma. Curr. Allergy Asthma Rep. 2011; 11:388–394. [PubMed: 21773747]
36. Crowe CR, et al. Critical role of IL-7RA in immunopathology of influenza infection. J. Immunol. Baltim. Md 1950. 2009; 183:5301–5310.
37. Stoppelenburg AJ, et al. Local IL-7A potentiates early neutrophil recruitment to the respiratory tract during severe RSV infection. PloS One. 2013; 8:e78461. [PubMed: 24194936]
38. Faber TE, Groen H, Welfing M, Jansen KJG, Bont LJ. Specific increase in local IL-7 production during recovery from primary RSV bronchiolitis. J. Med. Virol. 2012; 84:1084–1088. [PubMed: 22585726]
39. Chen Y, et al. Stimulation of Airway Mucin Gene Expression by Interleukin (IL)-7 through IL-Paracrine/Autocrine Loop. J. Biol. Chem. 2003; 278:17036–17043. [PubMed: 12624114]

40. English L, et al. Autophagy enhances the presentation of endogenous viral antigens on MHC class I molecules during HSV- infection. Nat. Immunol. 2009; 10:480–487. [PubMed: 19305394]
41. Chemali M, Radtke K, Desjardins M, English L. Alternative pathways for MHC class I presentation: a new function for autophagy. Cell. Mol. Life Sci. 2011; 68:1533–1541. [PubMed: 21390546]
42. Pua HH, Dzhagalov I, Chuck M, Mizushima N, He Y-W. A critical role for the autophagy gene Atg5 in T cell survival and proliferation. J. Exp. Med. 2007; 204:25–31. [PubMed: 17190837]
43. Pua HH, Guo J, Komatsu M, He Y-W. Autophagy is essential for mitochondrial clearance in mature T lymphocytes. J. Immunol. Baltim. Md 1950. 2009; 182:4046–4055.
44. Heid ME, et al. Mitochondrial reactive oxygen species induces NLRP3-dependent lysosomal damage and inflammasome activation. J. Immunol. Baltim. Md 1950. 2013; 191:5230–5238.
45. Zhou R, Yazdi AS, Menu P, Tschopp J. A role for mitochondria in NLRP3 inflammasome activation. Nature. 2011; 469:221–225. [PubMed: 21124315]
46. Smith CM, et al. Ciliary dyskinesia is an early feature of respiratory syncytial virus infection. Eur. Respir. J. 2013
47. Ogata M, et al. Autophagy is activated for cell survival after endoplasmic reticulum stress. Mol. Cell. Biol. 2006; 26:9220–9231. [PubMed: 17030611]
48. Yorimitsu T, Nair U, Yang Z, Klionsky DJ. Endoplasmic reticulum stress triggers autophagy. J. Biol. Chem. 2006; 281:30299–30304. [PubMed: 16901900]
49. Castillo K, et al. BAX inhibitor- regulates autophagy by controlling the IRE1α branch of the unfolded protein response. EMBO J. 2011; 30:4465–4478. [PubMed: 21926971]
50. Miller AL, Bowlin TL, Lukacs NW. Respiratory syncytial virus-induced chemokine production: linking viral replication to chemokine production in vitro and in vivo. J. Infect. Dis. 2004; 189:1419–1430. [PubMed: 15073679]

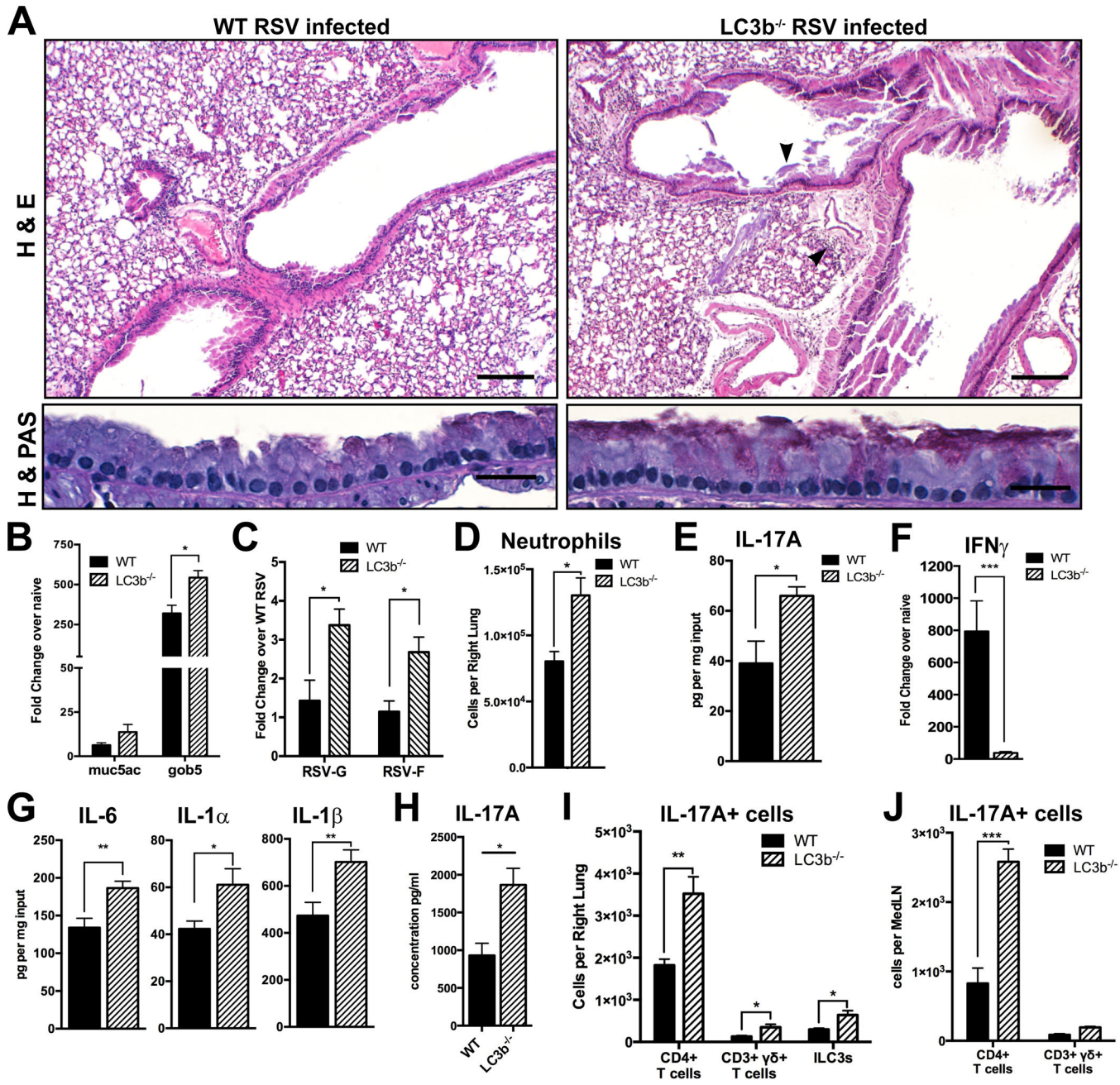

Figure 1. LC3b$^{-/-}$ mice develop increased lung pathology upon RSV infection

A) Lung sections of WT or LC3b$^{-/-}$ mice, 8 days post-infection (DPI) with RSV, were stained with either haematoxylin and eosin (H & E, upper panels) or periodic acid schiff and haematoxylin (H & PAS, lower panels) to visualize mucus along airway epithelium. Arrows indicate inflamed bronchiole (top) and perivascular granulocyte infiltration (bottom). Scale bars = 500μm for upper panels, 20μm for lower panels. B) Lung mRNA expression of *muc5ac* and *gob5* at 8 DPI was obtained by qPCR, compared to naïve controls. C) mRNA transcripts from lungs, encoding RSV-G and –F proteins, were measured by qPCR and normalized to values of WT RSV-infected lung samples. D) Neutrophils in right lungs of

WT and LC3b$^{-/-}$ mice at 8 DPI were quantified by flow cytometry, following enzymatic digestion of lungs. Total granulocytes were gated CD11b^{hi} CD11c^{lo} SSC^{hi} Auto^{lo}, with neutrophils gated Ly6G^{hi} Ly6C^{+}. E) IL-17a concentrations in whole lung lysates, normalized to protein input, were measured by Bioplex assay. F) Lung IFNγ values were obtained by qPCR. Fold change values were calculated relative to naïve control mice. G) Concentrations of IL-6, IL-1α, and IL-1β were measured in whole lung lysates by Biopex assay, normalized to protein input. H). Culture supernatant concentrations of IL-17a in RSV-restimulated lymph node cultures was measured at 48 hours by Bioplex assay. I) Single-cell suspensions prepared from enzymatically-digested lungs were treated with Golgi Stop, stimulated in culture with 10ng/ml PMA and 1μg/ml Ionomycin for 5 hours, followed by surface/intracellular staining and analysis by flow cytometry. CD4+ T cells were gated CD45^{+} CD3^{+} CD4^{+} γδ^{-}, γδ T cells gated CD45^{+} CD3^{+} γδ^{+}, and ILC3s gated CD45^{+} Lineage^{-} Thy1.2^{+} RORγt^{+}. J) Single-cell preparations from MedLNs were stained and gated as in (I). Results are representative of at least two independent experiments, n≥4 mice per group. *p≤0.05, **p≤0.01, ***p≤0.001.

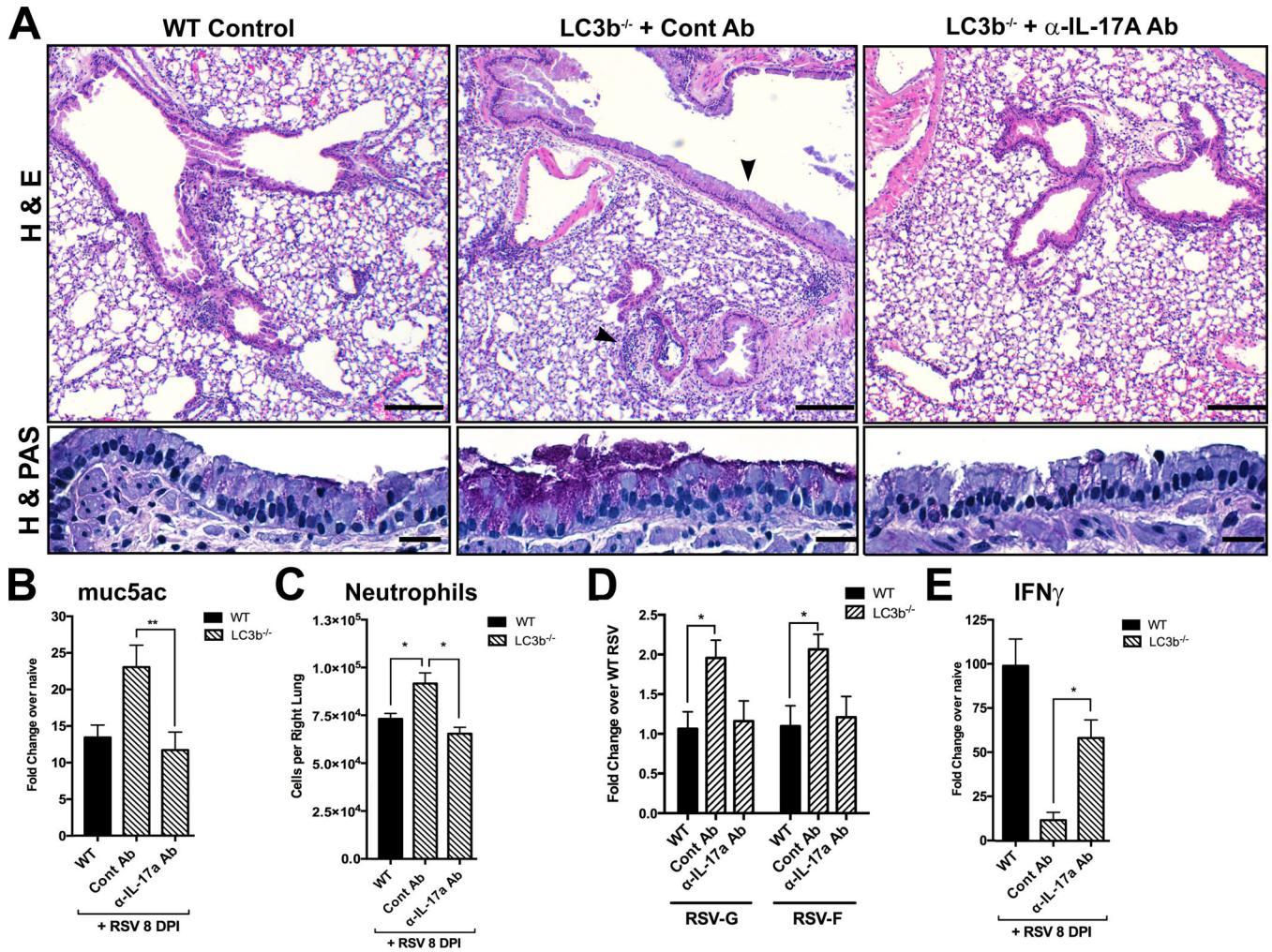

Figure 2. Increased RSV-induced lung pathology in LC3b$^{-/-}$ mice is IL-17a-dependent

LC3b$^{-/-}$ mice were treated with 2.5mg non-specific control antibody, or polyclonal antibody to mouse IL-17a, immediately prior to RSV infection and at days 2, 4, and 6 post-infection. A) Lungs were harvested at 8 DPI, sectioned, and stained with haematoxylin and eosin (H & E) or haematoxylin and periodic acid schiff (H & PAS) to visualize mucus. Arrows indicate inflamed bronchiole (top) and perivascular granulocyte infiltration (bottom). Scale bars = 500μm on upper panels, 20μm on lower panels. B) Lung expression of the mucin gene *muc5ac* was measured at 8 DPI by qPCR, relative to naïve controls. C) Neutrophils were quantified by flow cytometric analysis of enzymatically-digested lungs, 8 DPI. Neutrophils were gated as indicated in Figure 1. D) Lung mRNA expression encoding RSV-G and RSV-F was assessed at 8 DPI, relative to RSV-infected WT. E) Lung IFNγ expression was measured at 8 DPI by qPCR. Results are representative of three independent experiments, n≥4 mice per group. *p≤0.05, **p≤0.01, ***p≤0.001.

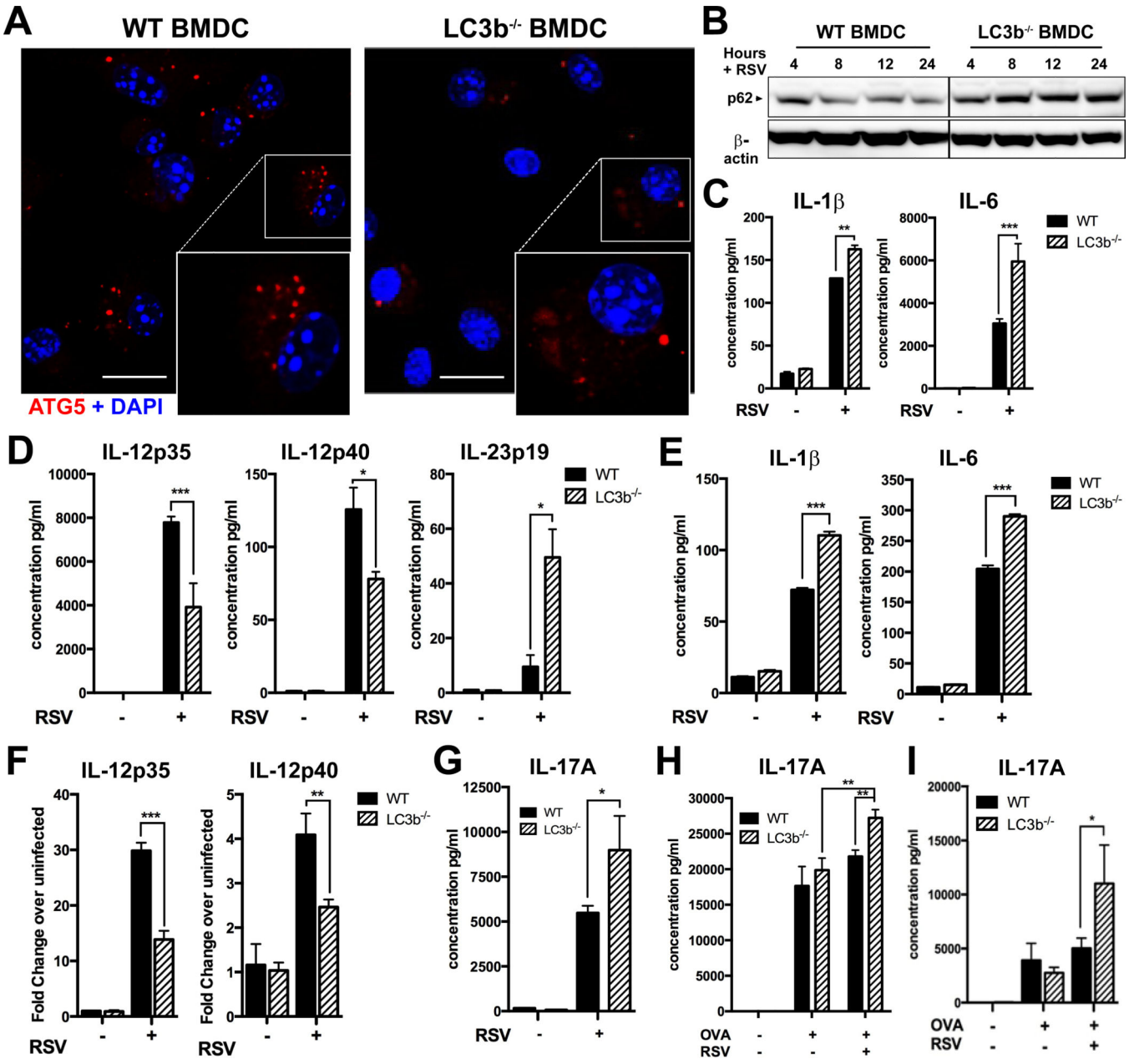

Figure 3. Altered autophagic flux, innate cytokine production, and elicitation of CD4+ T cell IL-17a production by LC3b$^{-/-}$ DCs in response to RSV

A) Bone marrow-derived DCs (BMDCs) were cultured from naïve WT or LC3b$^{-/-}$ mice, then infected for 4 hours with RSV. Cells were fixed, stained with DAPI and fluorescent antibody to ATG5, and imaged by confocal microscopy. Scale bars = 10μm. B) BMDCs were cultured and infected with RSV, followed by harvest at 4, 8, 12, and 24 hours post-infection. Whole cell lysates were run on SDS-PAGE gels, followed by membrane transfer and immunoblot for p62 or β-actin as indicated. C) Cell supernatants from BMDCs infected with 1:1 MOI RSV for 48 hours, analyzed by Bioplex assay. D) BMDCs were infected as above, harvested at 24 hours post-infection, and gene expression analyzed by qPCR. E) Lung-resident CD11c^{hi} Auto^{lo} CD11b^{+} lamina propria DCs (CD11b^{+} LP DCs) were flow-

sorted from enzymatically-digested lungs of naïve WT and LC3b$^{-/-}$ mice. Cells were infected *ex vivo* with 1:1 MOI RSV, and cell supernatants harvested at 48 hours post-infection by Bioplex assay. F) Lung-resident CD11b^{+} LP DCs were isolated and infected with RSV as previously described, followed by gene expression analysis by qPCR at 24 hours post-infection. G) CD4+ T cells were purified from mediastinal lymph nodes of RSV-infected C57Bl/6 mice, 8 days post-infection. Cells were plated at a 10:1 ratio over WT or LC3b$^{-/-}$ BMDCs, infected 2 hours previously with 1:1 MOI RSV. Culture supernatant IL-17a concentrations were measured at 48 hours by Bioplex assay. WT or LC3b$^{-/-}$ BMDCs (H) or CD11b^{+} LP DCs (I) were pulsed with whole ovalbumin protein in the presence or absence of 1:1 MOI RSV, followed by the addition of 10:1 purified splenic OT-II CD4+ T cells. Culture supernatant IL-17a concentrations were measured at 48 hours by Bioplex assay. All results are representative of at least three independent experiments. *p≤0.05, **p≤0.01, ***p≤0.001.

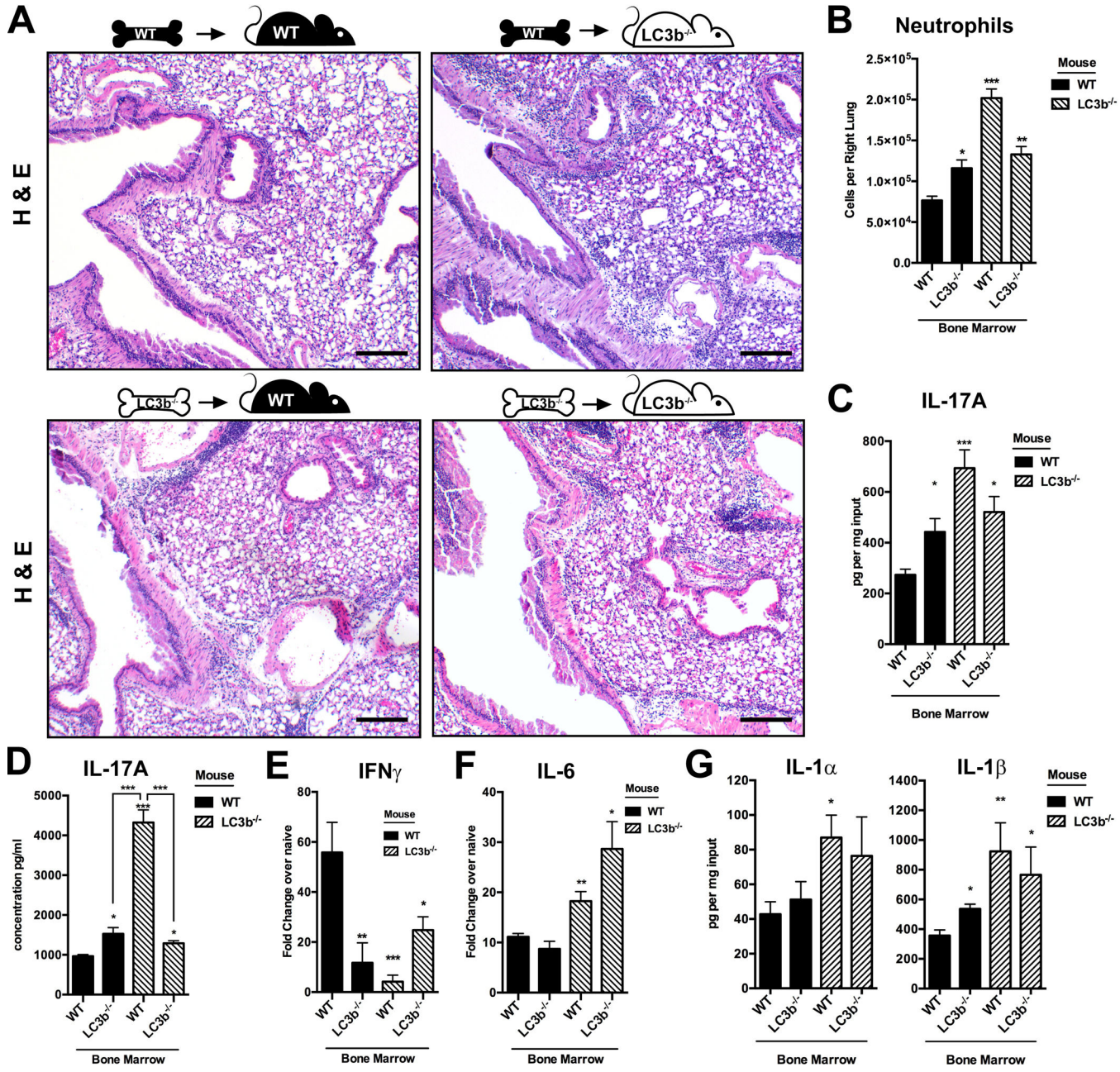

Figure 4. Both structural and hematopoietic LC3b deficiency contribute to increased lung pathology during RSV infection

WT and LC3b$^{-/-}$ mice were lethally irradiated and reconstituted with whole bone marrow from WT or LC3b$^{-/-}$ donors, as indicated. Chimeric mice were infected with RSV and sacrificed 8 days post-infection. A) Lung sections were stained with haematoxylin and eosin (H & E) to visualize inflammation. Scale bars = 500μm. B) Neutrophils were quantified from enzymatically-digested lungs by flow cytometry. Neutrophils were gated as indicated in Figure 1. C) Concentrations of IL-17a in whole lung lysates, normalized to protein input, were measured by Bioplex assay. D) IL-17a concentrations in RSV-restimulated MedLN cultures were measured at 48 hours by Bioplex assay. Lung mRNA expression of IFNγ (E)

and IL-6 (F) were measured by qPCR. G) Concentrations of IL-1α and IL-1β in whole lung lysates, normalized to protein input, were measured by Bioplex assay. Results are representative of three independent experiments, n≥4 mice per group. *p≤0.05, **p≤0.01, ***p≤0.001.

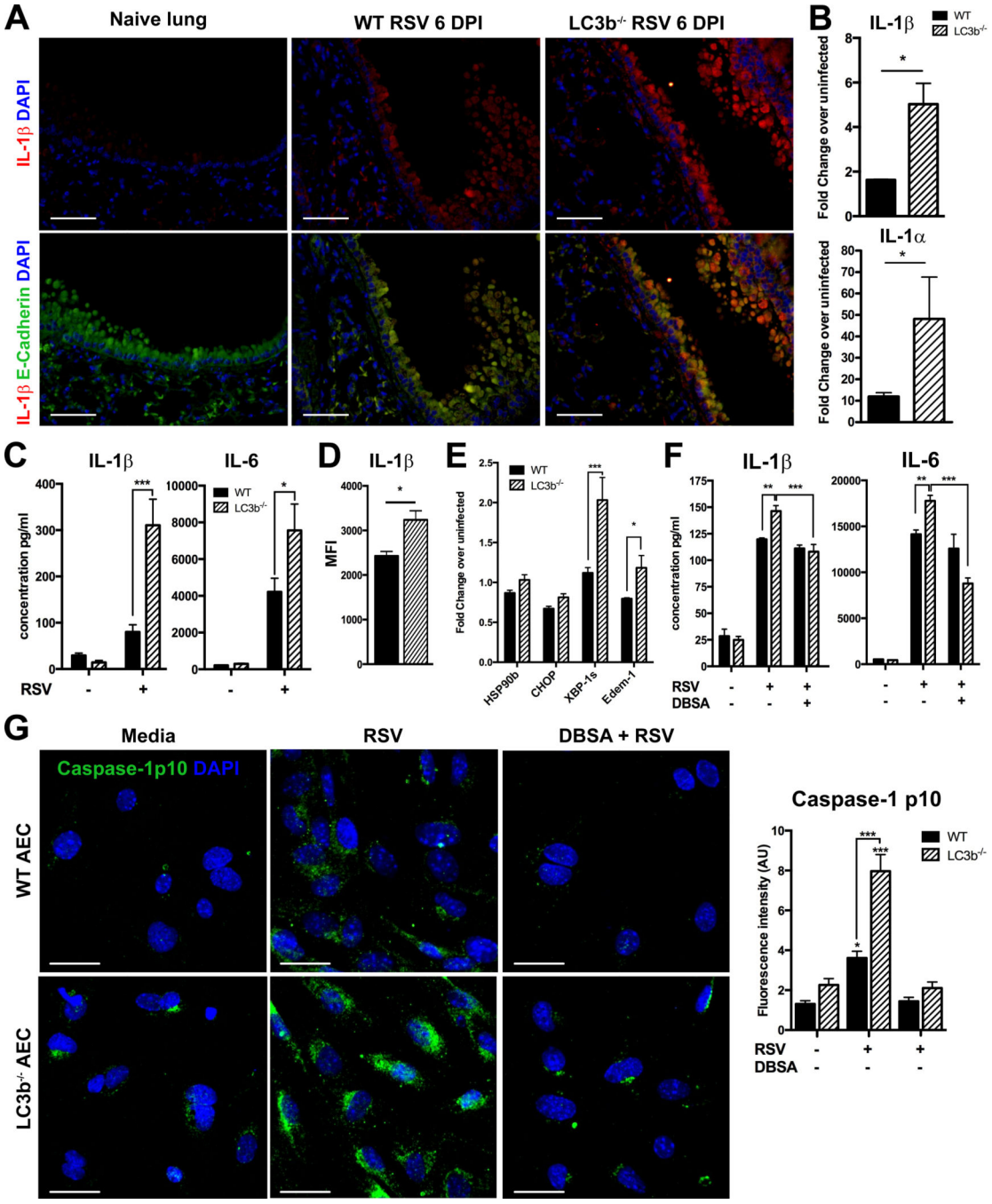

Figure 5. Increased pro-inflammatory cytokine production by LC3b$^{-/-}$ airway epithelial cells and lung macrophages upon RSV infection

A) Lung sections from WT and LC3b$^{-/-}$ mice, 6 days post-infection, were stained with antibodies to mouse IL-1β and E-cadherin. Sections were counterstained with DAPI and imaged on an Olympus BX43 fluorescent microscope. Scale bars = 40μm. (B,C) Airway epithelial cell (AEC) cultures were prepared from lungs of naïve WT or LC3b$^{-/-}$ mice, and infected with 1:1 MOI RSV. B) IL-1α and IL-1β expression was measured at 12 hours post-infection by qPCR, while C) IL-1β and IL-6 secretion was measured in culture supernatants at 24 hours by Bioplex assay. D) Single-cell suspensions prepared from enzymatically-

digested lungs were surface-stained, followed by intracellular IL-1β staining, and analyzed by flow cytometry. Lung macrophages were gated Auto^{hi} CD11b^{hi} F4/80^{+}. Dark histograms represent isotype control antibodies, light histograms anti-IL-1β antibody. E) Quantification of median fluorescence intensity staining of lung macrophages for IL-1β. E) mRNA transcripts of ER stress-associated genes HSP90, CHOP, Edem-1, and spliced XBP-1 were assessed in AECs at 12 hours post-infection by qPCR. (F) AECs were treated with the IRE-1α inhibitor 3,5-dibromosalicylaldehyde (DBSA) at 40μM, or the general ER stress inhibitor 4-phenlbutyrate (4-PBA) at 5mM, 30 minutes prior to 1:1 MOI RSV. Cell culture supernatants were assayed at 24 hours post-infection by Bioplex assay. G) AECs were infected for 12 hours with 1:1 MOI RSV, then fixed and stained with antibodies to the Caspase-1 p10 subunit and DAPI. Cells were imaged on a Nikon A1 confocal microscope. Fluorescence intensity per cell was measured and quantified using maximum intensity projections, using ImageJ software. Scale bars = 30μm. Results are representative of at least two independent experiments. *p≤0.05, **p≤0.01, ***p≤0.001.

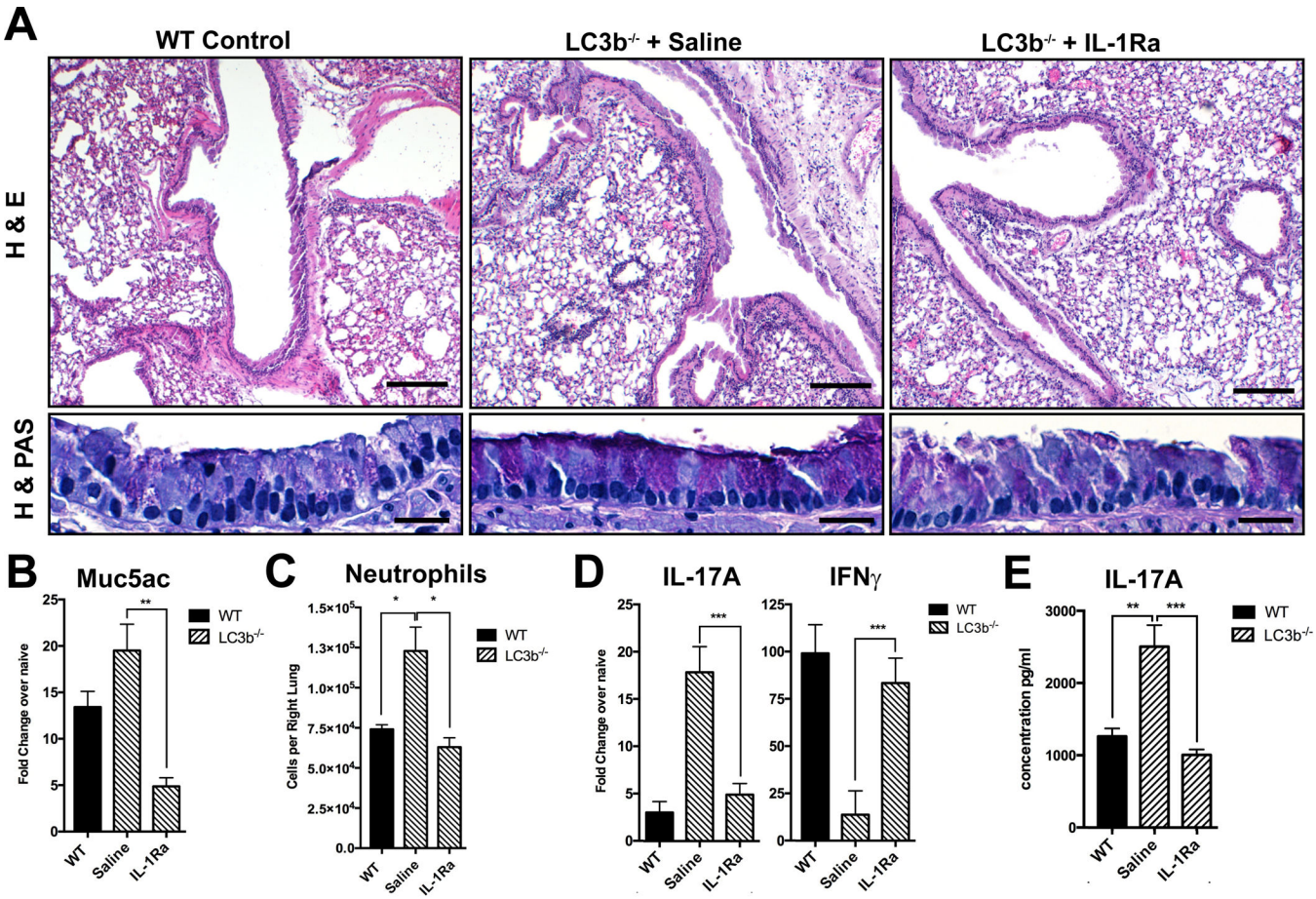

Figure 6. Increased IL-17a-dependent lung pathology in RSV-infected LC3b$^{-/-}$ mice is abrogated by blockade of IL-1 receptor signaling

LC3b$^{-/-}$ mice were injected I.P. with 25mg/kg mouse IL-1 receptor antagonist (IL-1Ra) immediately prior to RSV infection, then treated once daily until sacrificed at 8 days post-infection. A) Lung sections were stained with haematoxylin and eosin (H & E) or haematoxylin and periodic acid schiff (H & PAS) to visualize mucus. Scale bars = 100μm on upper panels, 20μm on lower panels. B) Lung expression of *muc5ac* was measured by qPCR. C) Neutrophils were quantified in enzymatically-digested lung tissue by flow cytometry, using cell surface antigens detailed in Figure 1. D) Expression of IL-17a and IFNγ were measured in lungs by qPCR. E) Single-cell suspensions prepared from mediastinal lymph nodes were restimulated in culture with RSV. IL-17a concentrations in supernatants were measured at 48 hours post-infection by Bioplex assay. Results are representative of two independent experiments, n≥5 mice per group. *p≤0.05, **p≤0.01, ***p≤0.001.

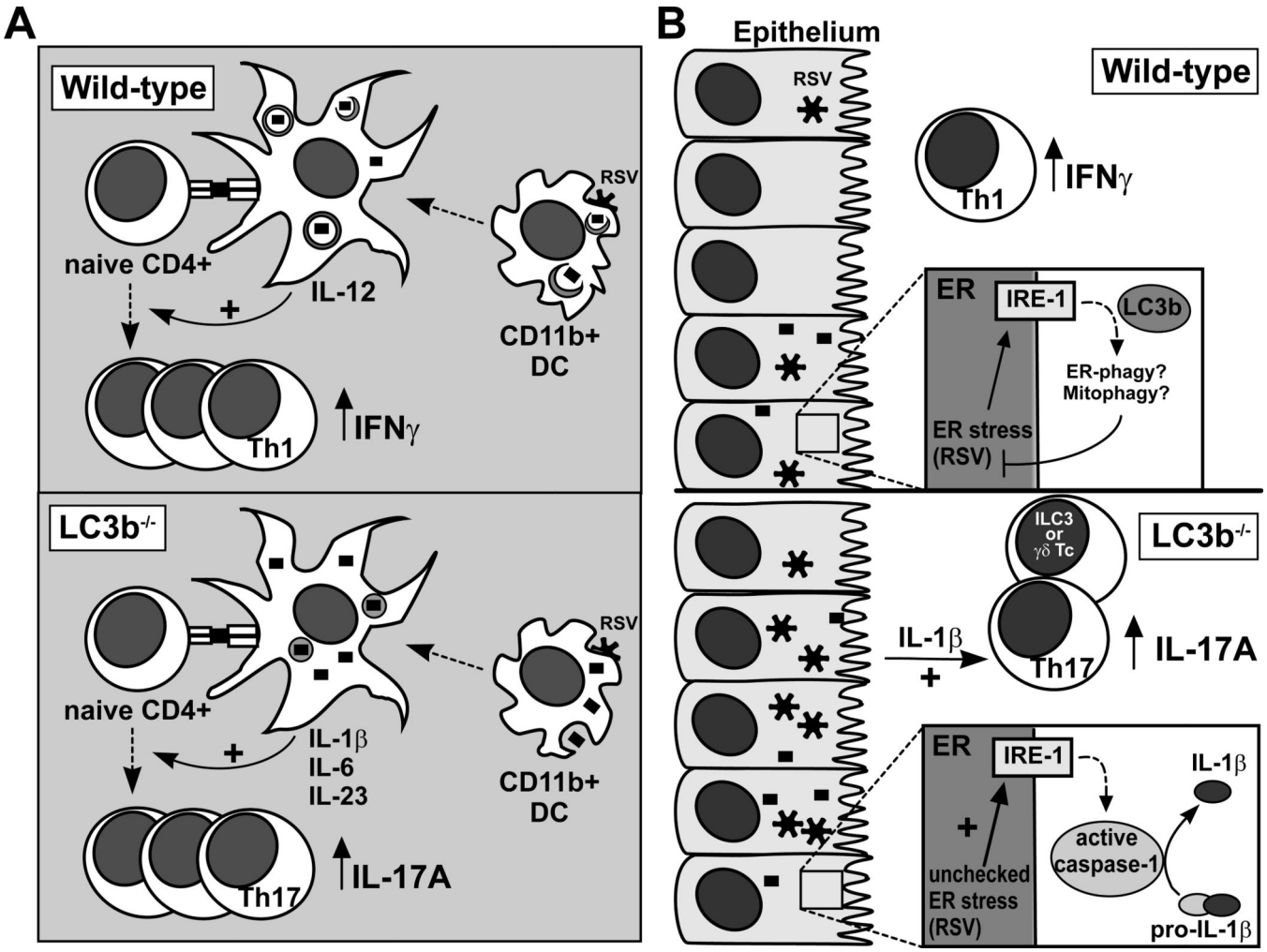

Figure 7. Proposed mechanisms of the induction and maintenance of CD4+ T cell responses to RSV in wild-type or LC3b$^{-/-}$ mice

A) Upon detection of RSV by WT lung DCs, rapid induction of autophagy facilitates IL-12 production, ultimately promoting the development of a Th1 response by RSV-reactive CD4+ T cells. In contrast, LC3b$^{-/-}$ DCs fail to upregulate autophagy upon encountering RSV, resulting in the production of IL-1β, IL-6, and IL-23. This cytokine environment skews RSV-reactive CD4+ T cells toward a Th17 phenotype. B) RSV-infected lung epithelial cells upregulate signaling through the ER stress sensor IRE-1, potentially triggering LC3b-dependent autophagosomal degradation of ER and damaged mitochondria, thereby alleviating RSV-induced stress and minimizing IL-1β production. In the absence of LC3b expression, RSV-infected epithelial cells experience increased IRE-1 signaling owing to unchecked ER stress, resulting in caspase-1 cleavage and mature IL-1β production. This enhanced IL-1β secretion stimulates further IL-17a production from CD4+ effector T cells through IL-1 receptor signaling.